

Evidence that channels below 1 pS cause the volume-sensitive chloride conductance in T84 cells

Melisa W.Y. Ho, Marek Duszyk, Andrew S. French *

Department of Physiology, University of Alberta, 7-55 Medical Sciences Building, Edmonton, Alberta T6G 2H7, Canada

(Received 23 September 1993)

Abstract

The volume-activated chloride current of T84 human colonic cells was studied using the whole-cell patch clamp. The current appeared reliably with a mild osmotic gradient and in the absence of intracellular ATP. It reversed at the chloride equilibrium potential and was blocked by the chloride channel blocker DIDS. Development of the current was accompanied by an increase in the current noise variance, typical of increasing ion channel open probability. Noise variance was always well-fitted by a double Lorentzian relationship with corner frequencies at ~ 1.7 Hz and ~ 60 Hz. The increase in variance during development of the volume-sensitive current was mostly due to an increase in the high frequency component. The relationship between noise variance and membrane current was well-fitted by a relationship with a single channel conductance of ~ 0.2 pS.

Key words: Epithelium; Noise analysis; Chloride channel; Cell swelling

1. Introduction

Ionic currents associated with cell swelling have been described in a variety of epithelial cells [1]. In whole-cell patch clamp recordings, they can be induced by an osmotic gradient that favors water entry into the cell. Increased membrane chloride conductance has been associated with such volume-sensitive currents in human airway epithelium [15,20], the human T84 colonic epithelial cell line [20,24], human I407 small intestine epithelial cells [10], human colon HT₂₉ cells [11], murine T-lymphocytes [12], and canine cardiac cells [22].

Clear separation of volume effects from other intracellular signals has not always been possible. Epithelial cells contain a variety of chloride channels and these can be affected by cyclic AMP, calcium and membrane potential, as well as volume [1]. Cross-sensitivity to volume and voltage has been reported in several cases, with depolarization causing inactivation [10,15,20,24] although other volume-sensitive currents were not inactivated by voltage [12,22]. There is also an associa-

tion between volume-sensitivity and intracellular ATP levels. ATP was reported to be essential for development of the volume-sensitive current in T-lymphocytes [12], it cross-reacted with cell swelling, calcium, and other agents in HT₂₉ cells [11], and was present in the pipet solution during several other studies [10,15,24]. However, ATP has also been reported to activate a small chloride channel via a membrane-bound cGMP-dependent protein kinase, that was not related to cell swelling [13].

A wide variety of chloride single-channel conductances have been found in epithelia. For example, there are at least five different types of chloride channels in human airway epithelia [2] including channels of only 4–5 pS [4,23]. The swelling-induced current in epithelia has been most commonly associated with an outwardly rectifying chloride channel of about 50 pS conductance [10,15,20,24], based on the outwardly rectifying nature of the current, observations of discrete current jumps in whole-cell records [24] and single channel records from swollen cells [20]. However, noise analysis of the volume-activated current in T-lymphocytes indicated that much smaller channels of ~ 2 pS were responsible for the current [12], and the chloride channels in HT₂₉ cells were reported to be too small to be resolved by single channel recording [11]. A

* Corresponding author. Fax: +1 (403) 4928915, E-mail: afrench@vm.ucs.ualberta.ca.

volume-activated current has also been linked to the P-glycoprotein, which creates chloride channels distinct from the other known chloride currents [7].

In the present work we re-examined the volume-sensitive chloride current in T84 cells. The current appeared reliably under an osmotic gradient and could be prevented by removal of the gradient. Noise analysis of the current variance gave a consistent estimate of ~ 0.2 pS for the single channel conductance, suggesting that the volume-sensitive current is due to a high density of very small channels that have not been identified previously.

2. Materials and methods

T84 cells, obtained from ATCC (American Type Culture Collection, Rockville, MD), were maintained in Dulbecco's modified Eagle's medium with Ham's nutrient mixture F-12 (Sigma), containing NaHCO_3 (7.5% W/V). Growth medium was supplemented with penicillin (100 U/ml), streptomycin (75 U/ml), gentamycin (0.5 mg/ml) and 5% fetal bovine serum (Sigma). The culture was kept at 37°C in a humidified 5% CO_2 -95% air incubator and the medium was changed every two days. Confluent monolayers were subcultured by treatment with 50 $\mu\text{g}/\text{ml}$ trypsin in Ca^{2+} - and Mg^{2+} -free Hank's buffered salt solution. Cells for study (passage 65–85) were plated at a density of $1 \cdot 10^4$ cells/ml in 35 mm dishes and were used within 2 days after seeding.

For electrical recording, cells were placed in Ringer solution, with three washes. Normal Ringer contained (mM): 140 NaCl, 5 KCl, 2 CaCl_2 , 1 MgCl_2 , 10 Hepes (pH 7.3). Whole-cell patch clamp experiments were performed on single, isolated cells using pipets made from thin-walled borosilicate glass with a two-stage vertical puller. Pipet tips were fire polished to ~ 0.5 μm diameter (2–5 M Ω) immediately before use. Normal pipet solution contained (mM): KCl 140, NaCl 5, CaCl_2 0.5, MgCl_2 2, EGTA 5, Hepes 10 (pH 7.3) (free calcium concentration 7.3 nM). Hypertonic Ringer solution or hypertonic pipet solution contained an additional 20 mM sucrose. The chloride channel blocker DIDS (4,4'-diisothiocyanatostilbene-2,2'-disulfonic acid, Sigma) was dissolved in Ringer before being applied.

Recording was performed by a List EPC-7 amplifier. For current–voltage relationships the voltage was controlled and the data gathered by a digital computer, using 12-bit digital-to-analog and analog-to-digital converters. For continuous recordings of membrane current versus time, the voltage was controlled by a constant voltage source and the current recording was stored on videotape using a 16-bit digitizer.

For membrane current noise analysis, whole cell

currents were low-pass filtered with a 9-pole, 300 Hz, active filter. The current was sampled at 1 ms intervals and digitized by a 12-bit analog-to-digital converter for storage on a computer disk. Data was processed in segments of 4096 sample points. To remove the current trend, each segment was fitted by a second-order polynomial in time, using linear regression. The fitted polynomial was then subtracted from the original data. Total variance was calculated from the mean of the squared residual current values. For Lorentzian fitting, each segment was processed by the fast Fourier transform and spectra from a series of segments were averaged. Spectra were fitted by a double Lorentzian function of the form:

$$\sigma^2 = \frac{S_1}{1 + (f/\theta_1)^2} + \frac{S_2}{1 + (f/\theta_2)^2} \quad (1)$$

where σ^2 is the total variance, S_1 , S_2 are the low frequency plateaux and θ_1 , θ_2 the corner frequencies of the two Lorentzian functions, and f is frequency [14]. Fitting was performed by the Levenberg-Marquardt general nonlinear fitting algorithm [17] over the range 0–180 Hz, where the filter output was 99–100% of the input. The variance of each Lorentzian component was obtained by integrating over frequency.

The single channel conductance of the time dependent current, γ , was obtained by fitting the noise variance versus membrane current relationship with:

$$\sigma^2 = \sigma_0^2 + I(V - E)\gamma - I^2/N \quad (2)$$

where σ_0^2 is the background variance, I is the total membrane current, V is the membrane potential, E is the reversal potential, and N is the number of channels [6,18]. This second-order polynomial in membrane current was fitted by linear regression, with the linear term giving an estimate of γ and the quadratic term an estimate of N . The open probability of the channels, P_o , was then calculated as a function of membrane current, I :

$$P_o = I/[N(V - E)\gamma] \quad (3)$$

3. Results

On forming the whole-cell configuration, with normal Ringer solution in the bath and hypertonic pipet solution, the cell membrane current was usually below the measurement noise level. A volume-sensitive current then appeared and grew approximately linearly with time. Typical current–voltage relationships for the total cell current during the first 7 min of a recording are shown in Fig. 1. Currents like this appeared reliably without the presence of ATP in the pipet. The reversal potential for the currents was always near zero, close to the chloride equilibrium potential and far

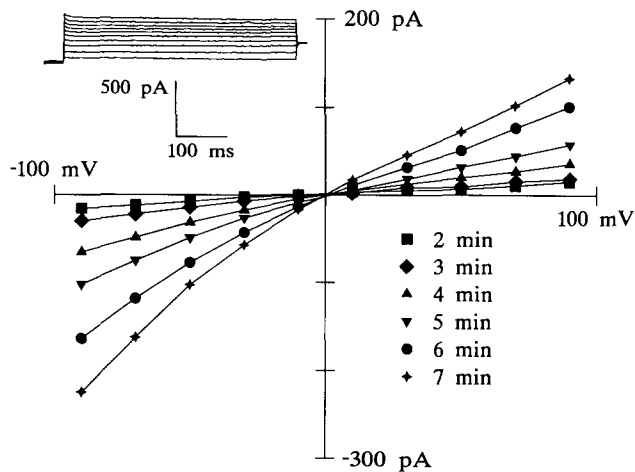


Fig. 1. Development of the volume-sensitive current after forming a whole-cell patch recording with normal bath Ringer and hypertonic pipet solution. Current-voltage relationships are shown for the total cell membrane current during the second to seventh minutes of the experiment. Note the inwardly rectifying nature of the current, and the reversal potential of zero at all times. Original current records for the seventh minute are shown in the inset. The holding potential was -40 mV and the cells were stepped to -100 mV initially to remove any voltage-dependent inactivation. The main plot was obtained from the mean current during the final 10 ms of such recordings.

from either the sodium or potassium equilibrium potentials. No evidence was seen for inactivation of the current during steps from the initial potential of -100 mV to more depolarized potentials. There was inward rectification throughout the development of the current.

During the appearance of the volume-sensitive current, cells visibly swelled and eventually became unstable. The swelling and the current could be prevented by raising the osmolarity of the bath solution. Fig. 2 shows mean current-voltage relationships after 4 min

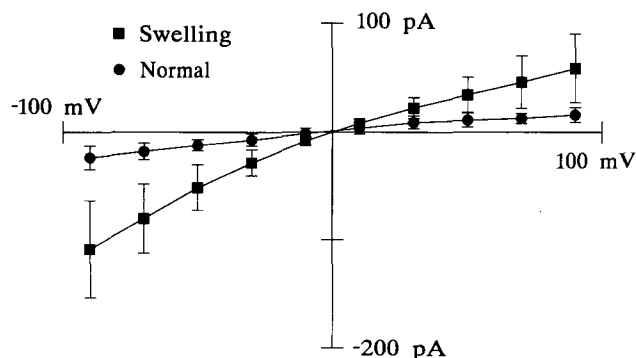


Fig. 2. The appearance of the volume-sensitive current could be prevented by reversing the osmotic gradient. Mean (\pm standard deviation) current-voltage plots are shown from four whole-cell recordings in normal saline and hypertonic pipet solution (squares) and four cells in hypertonic saline and normal pipet solution (circles). All recordings were made at 4 min after starting the experiments.

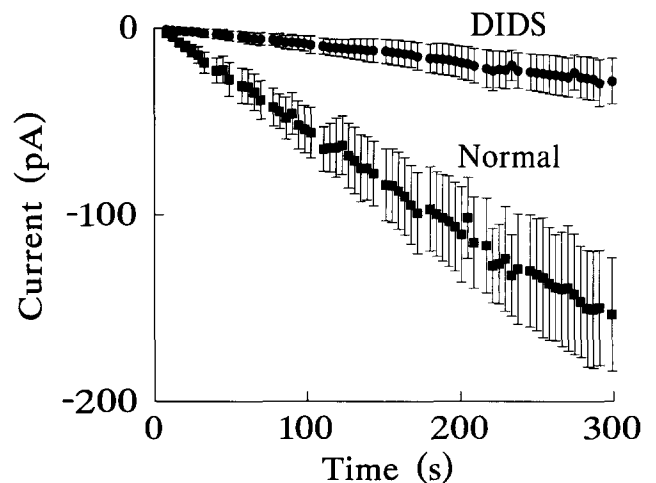


Fig. 3. The volume-sensitive current developed approximately linearly with time after forming the whole-cell patch and could be blocked by DIDS. Mean currents (\pm S.D.) at -60 mV holding potential are shown for 10 cells in normal saline (squares) and 7 cells in bath solution containing $20 \mu\text{M}$ DIDS (circles).

of whole-cell recording in two groups of cells. One group was in normal Ringer with hypertonic pipet solution, and the current grew as in Fig. 1. The other group was in saline containing an additional 20 mM sucrose, with normal pipet solution. These cells showed no detectable swelling or current development.

Because of the inwardly rectifying form of the current-voltage relationship, the detailed growth of the current and its noise variance were followed at a constant holding potential of -60 mV. The current grew approximately linearly with time after starting whole-cell recordings. Fig. 3 shows this relationship for the mean current from 10 different cells during the first 5 min of the experiments. Most of the current could be prevented by the chloride channel blocker DIDS ($20 \mu\text{M}$ in normal Ringer) as shown for seven different cells (Fig. 3) supporting the conclusion that the volume-sensitive current was carried by chloride ions.

Development of the volume-sensitive current was accompanied by an increase in the noise variance of the current record, as would be expected if the current were due to an increase in the open probability of a group of ion channels from an initially low value. In all cases this noise variance could be well-fitted by the double Lorentzian function of Eq. (1), and in all cases the contribution of the low frequency Lorentzian component remained approximately constant, while the growth of the high frequency component accounted for most of the increase in total variance. Fig. 4 shows the current noise spectra obtained during the first and fifth minutes of a typical experiment, together with portions of the actual current traces. During the first minute, the two components contributed variances of 0.46 pA^2

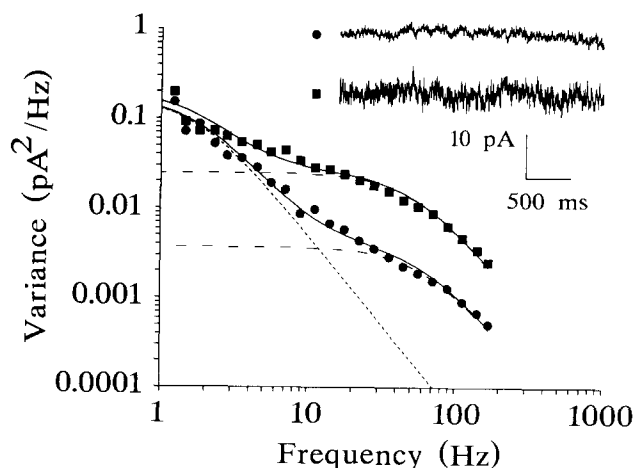


Fig. 4. Membrane noise variance increased during development of the volume-sensitive current. Noise spectra are shown for the first minute (circles) and fifth minute (squares) of a typical current recording. Both spectra were fitted by double Lorentzian functions (Eq. 1). For the first minute, the fitted parameters were: $S_1 = 0.17 \text{ pA}^2/\text{Hz}$, $\theta_1 = 1.7 \text{ Hz}$, $S_2 = 0.004 \text{ pA}^2/\text{Hz}$, $\theta_2 = 62.7 \text{ Hz}$. For the fifth minute, the fitted parameters were: $S_1 = 0.18 \text{ pA}^2/\text{Hz}$, $\theta_1 = 1.7 \text{ Hz}$, $S_2 = 0.025 \text{ pA}^2/\text{Hz}$, $\theta_2 = 53.2 \text{ Hz}$. The two low frequency components completely overlapped (short dashed lines). The high frequency components are shown as long dashed lines and the summed components as solid lines. Portions of the actual current records during these two periods are shown in the inset.

and 0.36 pA^2 with corner frequencies of 1.7 Hz and 62.7 Hz respectively. By the fifth minute the first component was unchanged but the second component had increased to 2.06 pA^2 , with a corner frequency of 53.2 Hz .

Similar Lorentzian fits were obtained from the first and fifth minutes of current development in 10 different cells. The mean ($\pm \text{S.D.}$) of the total current noise variance after 5 min was $1.93 \pm 0.51 \text{ pA}^2$ with the relative contribution of the second component being $70.4 \pm 0.06\%$. The mean corner frequencies of the two components were: $1.72 \pm 0.52 \text{ Hz}$ and $59.27 \pm 7.5 \text{ Hz}$, respectively. Therefore, the two Lorentzian components could be reliably identified and always made about the same relative contributions to the total noise variance. For the 10 experiments, the mean corner frequency of the low frequency component did not change significantly during 5 min of swelling ($1.75\text{--}1.72 \text{ Hz}$), but the corner frequency of the high frequency component decreased by about 25% ($76.06\text{--}59.27 \text{ Hz}$).

Eq. (2) predicts that the noise variance, σ^2 , produced by ion channels with changing open probability will be a second-order polynomial function of total membrane current, I . When the channels are totally closed ($P_o = 0$) or open ($P_o = 1$) the variance will be zero, but it will reach a maximum of I^2/N when $P_o = 0.5$. Noise variance did increase during development of the volume-sensitive current (Fig. 4) and its

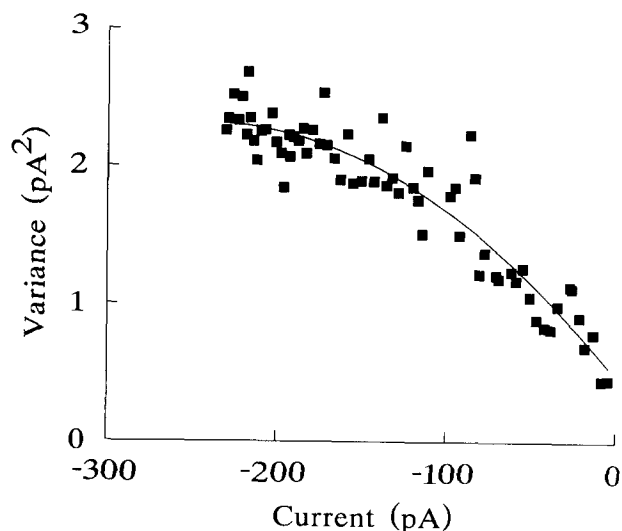


Fig. 5. Membrane noise variance as a function of total membrane current during the development of the volume-sensitive current. Squares show the original variance data. The fitted line is from Eq. (2) with parameters: $\sigma_0^2 = 0.48 \text{ pA}^2$, $\gamma = 0.25 \text{ pS}$, and $N = 32190$ channels.

dependence on the current could be approximated by Eq. (2). Fig. 5 shows this relationship for the first 5 min of one recording, with the fitted line corresponding to 32190 channels of 0.25 pS conductance. Similar measurements were made on 10 different cells, with mean parameters of: $\sigma_0^2 = 0.43 \pm 0.23 \text{ pA}^2$, $\gamma = 0.20 \pm 0.04 \text{ pS}$, and $N = 89000\text{--}98000$ channels. During the experiments with $20 \mu\text{M}$ DIDS in the bath, the total noise variance did not exceed 0.5 pA^2 , close to the background variance.

The open probabilities of the channels were calcu-

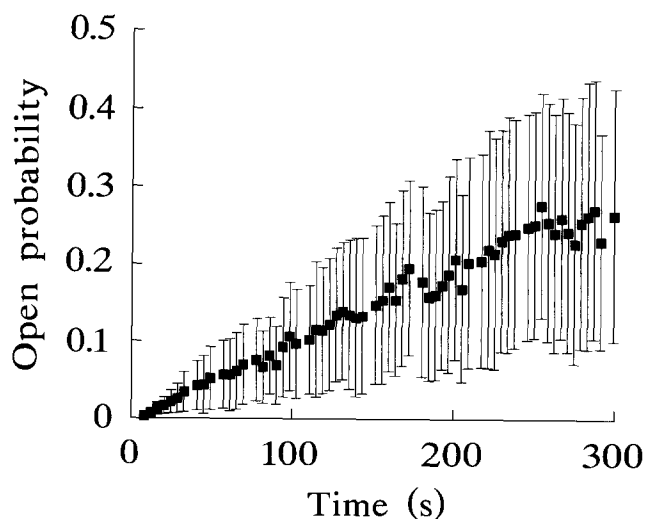


Fig. 6. Calculated open probability as a function of time after forming the whole cell patch. Mean ($\pm \text{S.D.}$) values are shown for the same 10 cells as in Fig. 3.

lated as functions of time from Eq. (3) during each experiment. Mean values of P_o versus time increased from near zero at the start of each experiment to a maximum of 0.25 after 5 min (Fig. 6). However, these data were quite variable, with some individual cells showing open probabilities of up to 0.6 after 5 min.

4. Discussion

The volume-sensitive current observed here had a similar amplitude and time course to the current reported before in T84 cells [24] and in T-lymphocytes [12]. It was also apparently carried by chloride ions, as indicated by the reversal potential and DIDS sensitivity. However, the electrical properties were quite different. The current that we observed was strongly inwardly rectifying and there was no indication of significant activation or inactivation with time after voltage steps, even with steps from -100 mV to 90 mV (Fig. 1). Inwardly rectifying chloride channels have been reported before in epithelia, although with much larger conductances than found here [3,9].

Another important difference was the estimated single-channel conductance of the channels responsible for the volume-sensitive current. The earlier measurements on T84 cells suggested a conductance of ~ 50 – 75 pS. These estimates were based on the outward rectification of the current and the amplitudes of discrete shifts in whole cell currents resembling single-channel events [24], as well as cell-attached single-channel recordings from swollen cells [20]. However, there were similarities between the channels activated by volume changes and by voltage, and some of the channel recordings assumed that both voltage and swelling activated the same set of channels. Our estimate of 0.2 pS is closer to the value of ~ 2 pS obtained by noise analysis in T-lymphocytes [12], and is compatible with the finding that swelling-induced chloride channels were too small to be resolved in HT₂₉ cells [11].

If the current is carried by such small channels, then the required channel density is high. Our analysis gave an estimate of $\sim 90\,000$ per cell. Using an average cell diameter of $20\ \mu\text{m}$ gives a density of ~ 70 channels/ μm^2 . Although quite high, this figure is within the known range of ion channel densities and much lower than the estimated density of $10\,000$ channels/ μm^2 estimated for acetyl choline channels at the motor endplate [8]. Verification of the existence of such small and densely packed channels by single-channel recording would be difficult. However, the estimates obtained here from noise analysis were consistent, and noise analysis has previously predicted the presence of small channels in epithelia that were later found by single-channel analysis [4,23]. If the present estimates are correct, the volume-sensitive channels

probably represent the most common ion channels in the cell membrane and a significant fraction of the total membrane proteins.

The cause of the double Lorentzian characteristic of the current noise is not yet known. In general, a double Lorentzian function may be due to the presence of two ion channels or to a single channel which spends significant amounts of time in several different open or closed states. The variance of the low frequency component did not increase during the development of the volume-sensitive current, its corner frequency was stable, and its mean amplitude after 5 min ($0.55\ \text{pA}^2$) was similar to the time invariant component of the total current variance ($\sigma_0^2 = 0.43\ \text{pA}^2$). These data could mean that the low frequency component was due to a population of channels that were partially open at the start of each experiment and remained unaffected by the development of the volume-sensitive current.

However, total membrane current at the start of each experiment was near zero (Fig. 3), so it seems more likely that only one population of channels with complex kinetics was responsible for the volume-activated current. If the high frequency component of the Lorentzian were due to a separate group of channels, the 25% decrease in its corner frequency (76 – 60 Hz) would correspond to an increase in mean open time from 2.1 to 2.7 ms. Alternatively, if the two Lorentzian components were due to a single group of channels with more complex kinetics, their relative changes in amplitude and corner frequency would represent shifts in the occupancy of channel states, but still include an increase in total channel open time.

Earlier work showed that the treatment of larger epithelial chloride channels by the stilbene derivatives DNDS [19] and SITS [16] caused a flickery block that was associated with reductions in channel open times. However, we did not observe any increases in total current variance or Lorentzian noise during the experiments with DIDS blockade.

One difference between our experiments and some earlier measurements of volume-sensitive currents was the absence of ATP in the pipet during our recordings. It seems possible that ATP is not essential for producing the volume-sensitive current, but can stimulate the appearance of a separate current with a similar time course but different electrical characteristics. Nucleotides have complex relationships with epithelial ion channels. In addition to their role in phosphorylation, nucleotides activate the CFTR protein by direct binding [21] and CFTR has been reported to play a role in regulating the activity of the 50 pS outwardly rectifying chloride channels of epithelia [5]. In our experience, the discrete membrane fluctuations, characteristic of rectifying channels, were never seen in cells without ATP in the pipet, but the volume-sensitive current appeared reliably without ATP and produced noise

that was well-fitted by a channel conductance of about 0.2 pS.

5. Acknowledgements

This work was supported by the Medical Research Council of Canada, the Alberta Heritage Foundation for Medical Research, and the Canadian Cystic Fibrosis Foundation.

6. References

- [1] Anderson, M.P., Sheppard, D.N., Berger, H.A. and Welsh, M.J. (1992) *Am. J. Physiol.* 263, L1–L14.
- [2] Duszyk, M., French, A.S. and Man, S.F.P. (1989) *Can. J. Physiol. Pharmacol.* 67, 1362–1365.
- [3] Duszyk, M., French, A.S., Man, S.F.P. and Becker, A.B. (1991) *Eur. Biophys. J.* 20, 65–69.
- [4] Duszyk, M., French, A.S. and Man, S.F.P. (1992) *Biophys. J.* 61, 583–587.
- [5] Egan, M., Flotte, T., Afione, S., Solow, R., Zeitlin, P.L., Carter, B.J. and Guggino, W.B. (1992) *Nature* 358, 581–584.
- [6] Ehrenstein, G., Lecar, H. and Nossal, R. (1970) *J. Gen. Physiol.* 55, 119–133.
- [7] Gill, D.R., Hyde, S.C. and Higgins, C.F. (1992) *Nature* 355, 830–833.
- [8] Hille, B. (1984) *Ionic Channels of Excitable Membranes*. Sinauer, Sunderland, MA.
- [9] Hanrahan, J.W., Alles, W.P. and Lewis, S.A. (1985) *Proc. Natl. Acad. Sci. USA* 82, 7791–7795.
- [10] Kubo, M. and Okada, Y. (1992) *J. Physiol.* 456, 351–371.
- [11] Kunzelmann, K., Kubitz, R., Grolik, M., Warth, R. and Greger, R. (1992) *Pflügers Arch.* 421, 238–246.
- [12] Lewis, R.S., Ross, P.E. and Cahalan, M.D. (1993) *J. Gen. Physiol.* 101, 801–826.
- [13] Lin, M., Nairn, A.C. and Guggino, S.E. (1992) *Am. J. Physiol.* 262, C1304–C1312.
- [14] Lindemann, B. and Van Driessche, W. (1977) *Science* 195, 292–294.
- [15] McCann, J.D., Li, M. and Welsh, M.J. (1989) *J. Gen. Physiol.* 94, 1015–1036.
- [16] Nelson, D.J., Tang, J.M. and Palmer, L.G. (1984) *J. Membr. Biol.* 80, 81–89.
- [17] Press, W.H., Flannery, B.P., Teukolsky, S.A. and Vetterling, W.T. (1990) *Numerical Recipes in C*. Cambridge University Press, Cambridge, UK.
- [18] Sigworth, F.J. (1980) *J. Physiol.* 307, 97–129.
- [19] Singh A.K., Afink, G.B., Venglarik, C.J., Wang, R. and Bridges, R.J. (1991) *Am. J. Physiol.* 260, C51–C63.
- [20] Solc, C.K. and Wine, J.J. (1991) *Am. J. Physiol.* 261, C658–C674.
- [21] Travis, S.M., Carson, M.R., Ries, D.R. and Welsh, M.J. (1993) *J. Biol. Chem.* 268, 15336–15339.
- [22] Tseng, G.-N. (1992) *Am. J. Physiol.* 262, C1056–C1068.
- [23] Wilk-Blaszczak, M.A., French, A.S. and Man, S.F.P. (1992) *Biomed. Res.* 13, 143–148.
- [24] Worrell, R.T., Butt, A.G., Cliff, W.H. and Frizzell, R.A. (1989) *Am. J. Physiol.* 256, C1111–C1119.